

Preparation and Characterization of Thermoplastic Antistatic Polyurethane Synthesized by *In Situ* Polymerization

Changbing Li, Rongsheng Che, Jun Xiang, Jingxin Lei, Changlin Zhou

State Key Laboratory of Polymer Materials Engineering, Polymer Research Institute of Sichuan University, Chengdu 610065, China

Correspondence to: C. Li (E-mail: 344548698@qq.com)

ABSTRACT: Antistatic polyurethane (APU) is prepared by *in situ* polymerization of polyester glycol (PEL), 4,4'-diphenylmethane diisocyanate (MDI), 1,4-butanediol (BDO), and antistatic agent (AA) formed by dissolving sodium salts in polyethylene glycol (PEG). Comprehensive properties of the APU are investigated by the FT-IR, mechanical characterization, surface resistivity measurement, relative humidity (RH) study, and TGA, respectively. It is found that the surface resistivity of the APU can be effectively reduced to $10^{9.15} \Omega$, showing a good antistatic property. Moreover, the APU maintains a low surface resistivity ($\sim 10^{9.43} \Omega$) at the RH of 0.1%, revealing a non-RH-sensitive capacity of the APU. © 2013 Wiley Periodicals, Inc. *J. Appl. Polym. Sci.* **2014**, *131*, 39921.

KEYWORDS: applications; conducting polymers; elastomers; polyelectrolytes; properties and characterization

Received 29 June 2013; accepted 1 September 2013

DOI: 10.1002/app.39921

INTRODUCTION

Polyurethane (PU) is one of the six most important synthetic materials, which is segmented polymer built up from soft and hard segments. They possess not only a highly elastomeric behavior, but also a good abrasion resistance, chemical resistance, and high tensile strength.^{1,2} PU is a good electric insulator, because its surface resistivity ranges from 10^{11} to $10^{13} \Omega$. However, such a high surface resistivity likely produces static electricity, which is potentially disastrous upon discharge. Therefore, the antistatic problems of PU elastomer have attracted lots of attention since the 1960s, and some conductive or antistatic materials have been developed accordingly.³

Many studies have reported main methods to avoid or suppress static electricity which include: adding an antistatic agent;⁴ loading carbon black, metal powder, metal oxide, or inorganic salt;^{5–10} blending conductive polymer;^{11,12} surface modification.³ Unfortunately, several issues associated with the methods mentioned above have been clearly realized. Antistatic agents cannot endow the polymer with a persistently antistatic ability, and the relative humidity (RH) has strong effect on the surface resistivity of the polymer, which restricts their large applications. Conductive fillers suffer main problems of relatively high cost and filler migration or metal decay in the polymer matrix and surface, which would further limit their large scale applications in industry.¹³

Solid-polymer-electrolytes (SPEs) proposed by Wright,¹⁴ have received considerable attention because of the good ionic conductivity ability caused by the migration of metal ions. For the excellent ionic conductivity, SPEs are usually used in the field of high energy density and leak proof batteries.^{15,16} Commonly, poly(ethylene oxide)-based polymer electrolytes are studied intensively because of their excellent ability to solvate cations.^{17–20} In terms of the permanently ion-conductive ability and the light color of SPE-based antistatic agents, it seems that the use of ion-conductive SPEs as antistatic agents to improve antistatic capacity of polymer is a novel development, which can solve these problems produced by the conventional methods referred before. Recently, a number of relevant investigations regarding SPE-based antistatic composites obtained by conventional blend method have been studied.^{21–28} To the best of our knowledge, however, it seems that there have been no previous reports concerning the SPE-based antistatic PU prepared by *in situ* polymerization.

In this study, the APU was synthesized *via* copolymerizing antistatic agent (AA) with 4,4'-diphenylmethane diisocyanate (MDI), polyester glycol (PEL), and 1,4-butanediol (BDO) by using an *in situ* polymerization, taking account of the high conductivity, low price, and straightforward method of preparation. The effects of salts content, RH, and temperature on the surface resistivity of the APU were investigated. The antistatic materials have also been tested by Fourier transform infrared (FT-IR), mechanical characterization, and surface resistivity measurement.

EXPERIMENTAL

Materials

4,4'-Diphenylmethane diisocyanate (MDI) was supplied by Yantai Wanhua Polyurethanes Co. (Shandong, China). Polyester glycol (PEL) was kindly provided by Xing Yutian Chemical Co. (Qingdao, China). Polyethylene glycol (PEG, $M_w = 400, 800, 1500, 2000,$ and 4000 g/mol), 1,4-butanediol (BDO), and anhydrous salts ($\text{NaClO}_4, \text{KClO}_4, \text{LiClO}_4$) were all from Kelong Chemical Reagent Co. (Chengdu, China). PEL, PEG, and BDO were dried under vacuum for 2 h at 120°C before use, respectively. All above chemicals used in this experiment were analytically pure.

Preparation of the Antistatic Agent (AA)

Anhydrous salts were dried in a vacuum oven for 4 h at 100°C before use. Then the pre-determined amounts of sodium salts were added to PEG, and the mixture was stirred for approximately 1 h at 80°C .²⁵ The corresponding antistatic polyetherdiol agent (AA) was fabricated.

Synthesis of the PU

Set contents of MDI and PEL were added to a three-necked flask. Dibutyltin dilaurate (DBTL) was added as a catalyst when the temperature reached 80°C . The homogenous mixture was stirred vigorously for 2 h and then BDO was added to extend the chains. Subsequently, the pre-polymer was poured on a Teflon laboratory dish when the viscosity was high enough and heated at 100°C for 6 h in a vacuum.

Preparation of the APU

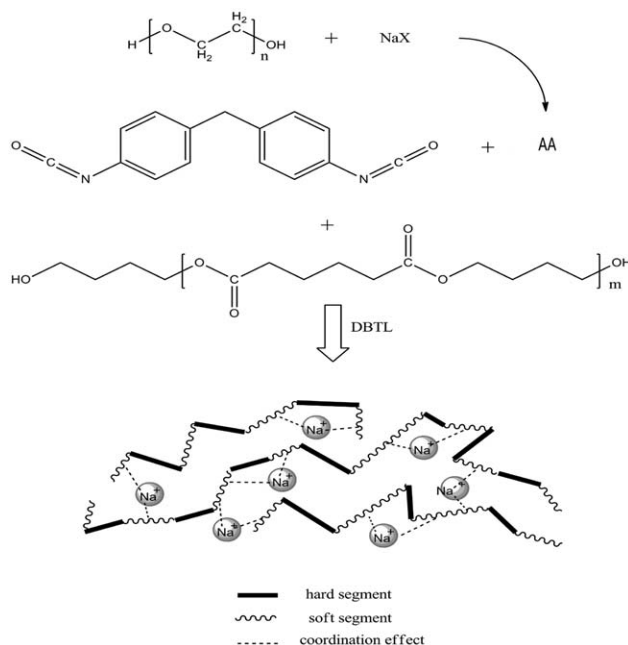
The APU was synthesized in a typical two-stage polyaddition process with the use of appropriate MDI, polydiol (PEL and AA) at the molar ratio of the $-\text{NCO}$ and $-\text{OH}$ functional groups maintained at 2 : 1. Dibutyltin dilaurate (DBTL) as a catalyst was added 0.1 wt % of PEL and AA. The pre-polymer was synthesized at 80°C for 2 h and then extended with BDO, with the molar ratio of 1 : 1. The chemical structure of the product polyurethane was shown in Scheme 1. Films were obtained by casting the melts onto a polytetrafluoroethylene (PTFE) substrate and heated at 100°C for 6 h.

Characterization

FT-IR Analysis. The samples were characterized by a Nicolet170sx FTIR spectrometer (Thermo Nicolet Corporation) with a resolution setting of 4 cm^{-1} . The scanning range was increased from 400 to 4000 cm^{-1} .

Mechanical Characterization. The tensile strength and elongation at break of the APU sample was tested with an Instron-4302 Mechanical Tester (America) at a constant tensile rate of 200 mm min^{-1} .

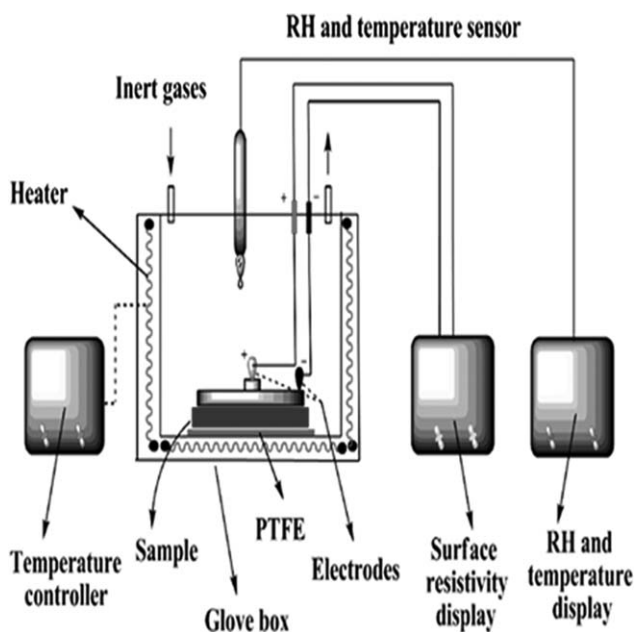
Surface Resistivity Measurement. The 1-mm-thick sheets of the antistatic polyurethane (APU) were prepared by compression molding at 160°C and were then used for conductivity measurements. The surface resistivity of the specimens was measured by using a surface resistivity meter (ZC64A, Shanghai, China). The environments of different RH and temperature for the surface resistivity tests were obtained with a special glove box that could be infused with high-purity nitrogen. The scheme of the instrument is shown in Scheme 2. Every environ-



Scheme 1. Schematic synthesis route of APU.

ment with different RH and temperature values was stabilized for more than 2 h before testing. The RH was detected by a thermohygrometer (TRH-AZ, provided by Shinyei Co., Tokyo, Japan).

TGA Analysis. A TA instrument SDT-Q600 thermal analyzer was utilized to study thermostability of the APU in air atmosphere, with a heating rate of $10^\circ\text{C min}^{-1}$ and *ca.* 10 mg of each sample. The specimens researched in this study were previously dried at 80°C for 3 h in a vacuum oven. All TGA curves were analyzed by a TA conventional analysis program.



Scheme 2. Scheme of the instrument for the surface resistivity test (PTFE = polytetrafluoroethylene).

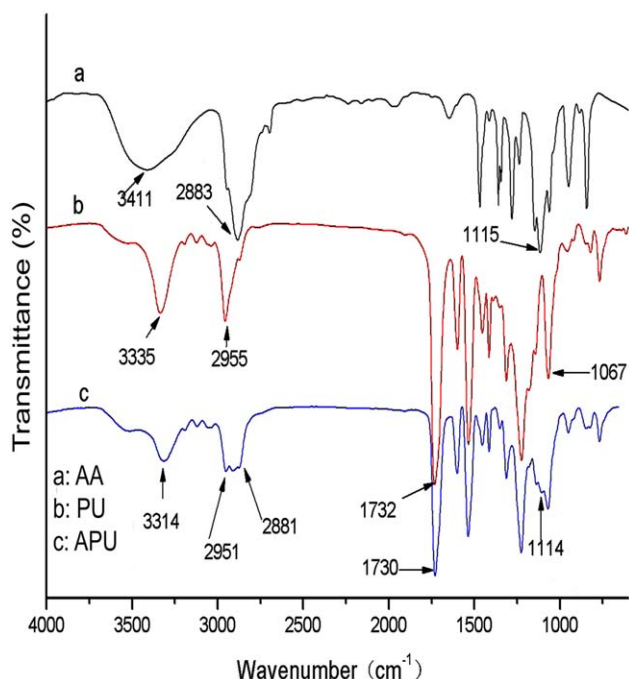


Figure 1. FT-IR of (a) AA, (b) PU, and (c) APU. [Color figure can be viewed in the online issue, which is available at wileyonlinelibrary.com.]

RESULTS AND DISCUSSION

FT-IR Measurement

The FT-IR spectra of AA, PU, and the APU are shown in Figure 1. As can be seen from Figure 1(a), a strong absorption band near 3411 cm^{-1} is detected, which is the characteristic absorption band of the $-\text{OH}$ asymmetric stretching of PEG end groups. In addition, the vibration of $-\text{CH}_2-$ around 2883 cm^{-1} and the characteristic absorption of $-\text{C}-\text{O}-\text{C}-$ at around 1115 cm^{-1} are also found in Figure 1(a). Figure 1(b) illustrates the FT-IR spectrum for the PU. The absorption peaks around 1067 , 1732 , 2955 , and 3335 cm^{-1} are assigned to the stretching vibration of the $-\text{C}-\text{O}-$, $-\text{C}=\text{O}$, $-\text{CH}_2-$, and $-\text{N}-\text{H}-$ groups, respectively. In comparison with Figure 1(b), in addition to the stretching vibration of the $-\text{C}=\text{O}$, $-\text{N}-\text{H}-$, and benzene ring, the characteristic absorption of $-\text{CH}_2-$ around 2881 cm^{-1} , originating from AA, are observed in Figure 1(c). Furthermore, in contrast to Figure 1(a), the absorption band at 1114 cm^{-1} originating from the $-\text{C}-\text{O}-\text{C}-$ stretching in PEG is also shown in Figure 1(c). However, the characteristic absorption band of the $-\text{OH}$ asymmetric stretching of PEG end groups vanishes, indicating that the APU is successfully synthesized by this method.

Electrical Properties

Effect of NaClO_4 Content and Various Salts Species on the Surface Resistance. Table I illustrates the relation between different NaClO_4 content and the surface resistance of the APU at 30°C and under a RH of 10%, which decreases with an increase in NaClO_4 content. However, the surface resistivity changes obviously when the NaClO_4 content is less than 9 wt %. With further increasing the NaClO_4 content, the surface resistivity decreases slowly. It seems that the NaClO_4 content of 9 wt % is the threshold value (critical point) for ion-conductive tunnels. Generally, the

Table I. Effect of NaClO_4 Content on the Surface Resistivity of the APU

| Sample code | Composition (wt %) | | Surface resistivity (Ω) |
|-------------|--------------------|----------------------|----------------------------------|
| | NaClO_4 | PEG ($M_w = 2000$) | |
| 1 | 0 | 100 | $10^{13.30}$ |
| 2 | 3 | 97 | $10^{11.42}$ |
| 3 | 6 | 94 | $10^{8.53}$ |
| 4 | 9 | 91 | $10^{7.82}$ |
| 5 | 12 | 88 | $10^{7.78}$ |
| 6 | 15 | 85 | $10^{7.76}$ |

number of charge carriers plays an important role on the ionic conductivity. In the hybrid films, NaClO_4 dissolves in polymer matrix and PEG, and thus the increase in NaClO_4 content enhances the number of carriers correspondingly. Therefore, the increase in the amount of NaClO_4 content is accompanied by an increase in the conductivity. The effect of the various salts species on the surface resistivity of the APU at 30°C and under a RH of 10% is shown in Table II. The polymer electrolytes complexed with KClO_4 exhibit higher ionic conductivity than those complexed with NaClO_4 and LiClO_4 . These differences of ionic conductivity depending on perchlorate salt species can be attributed to the difference in interaction energy of cation and anion. The cationic radius decrease gradually from K^+ , Na^+ to Li^+ in order. Larger cations have a longer distance between the positive and negative charge and require much less energy to separate them, originating from Coulomb's law: $E \sim e^2/d$, where e and $-e$ are charges carried by cation and anion and d is the distance between two charges. The lower interaction energy results in increased the concentration of "free" cation with an apparent inverse correlation with the cationic size, which improved the conductivity of the APU.

Effect of PEG with Different Molecular Weights (M_w 's) and AA Content on the Surface Resistance. Table III shows the dependence of the surface resistivity of the APU on PEG with

Table II. Effect of Various Salts Species on the Surface Resistivity of the APU

| Mass ratio (salt/AA) | Various salt | Surface resistivity (Ω) |
|----------------------|------------------|----------------------------------|
| 9/100 | KClO_4 | $10^{7.44}$ |
| | NaClO_4 | $10^{8.26}$ |
| | LiClO_4 | $10^{8.60}$ |

Table III. Effect of Molecular Weight (M_w 's) on the Surface Resistivity of the APU

| Molecular weight (M_w) | Mass ratio (NaClO_4/AA) | Surface resistivity (Ω) |
|----------------------------|---|----------------------------------|
| PEG 400 | 9/100 | 10^{13} |
| PEG 800 | 9/100 | $10^{9.54}$ |
| PEG 1500 | 9/100 | $10^{9.32}$ |
| PEG 2000 | 9/100 | $10^{9.24}$ |
| PEG 4000 | 9/100 | $10^{9.12}$ |

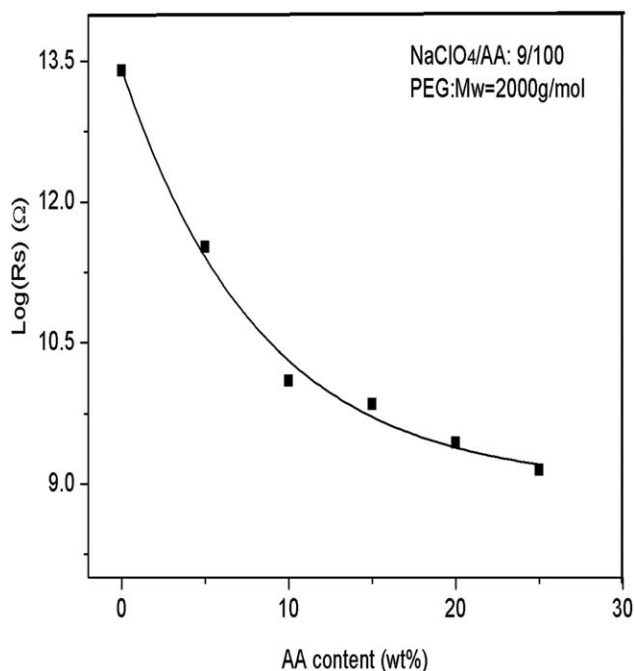


Figure 2. Surface resistivity of APU with AA content.

different M_w 's. When the value of temperature is held constant (30°C), an increase in M_w 's does bring about an increase in conductivity of the APU. The change in conductivity of the hybrid films is attributable to the change in carrier mobility. Under the identical temperature conditions, the long chains of $-\text{CH}_2\text{CH}_2\text{O}-$ of PEG are believed to form a loosely entangled network which does bring about appreciable improvement in carrier mobility, resulting in low surface resistivity of the APU. The effect of the AA content on surface resistivity of the APU is shown in Figure 2. It is clear that the surface resistance of the APU decreases with the AA content increase. When the AA content increases from 0 to 15 wt %, surface resistivity of the APU sharply decreases from $10^{13.5}$ to $10^{9.5}$ Ω. However, the surface resistivity does not exhibit substantial changes when the AA content is beyond 15 wt %. The ionic conductivity is closely proportional to the conductive networks numbers and the carrier mobility. The conductive networks numbers increase with an increase in AA content, which is instrumental to the migration of small ions. Further adding the AA content, however, the conductive networks increase unnoticeably although the surface resistivity of the APU decreases slightly, resulting in the surface resistivity values have not appreciable changes.

Effect of Temperature and Relative Humidity (RH) on Surface Resistivity. Figure 3 illustrates that the dependence of the surface resistivity of the APU on temperature under an RH of 10%. It is detected that the surface resistivity values depend on the temperature, changing from 10^{10} to $10^{6.6}$ Ω when the temperature alters from 21 to 78°C. The decline in the surface resistivity decreased with increasing temperature indicates typical features of an ion-conductive polymer. When the temperature increased, the ions possess more energy to easily break through the energy barrier of dissociation of the coordination effect

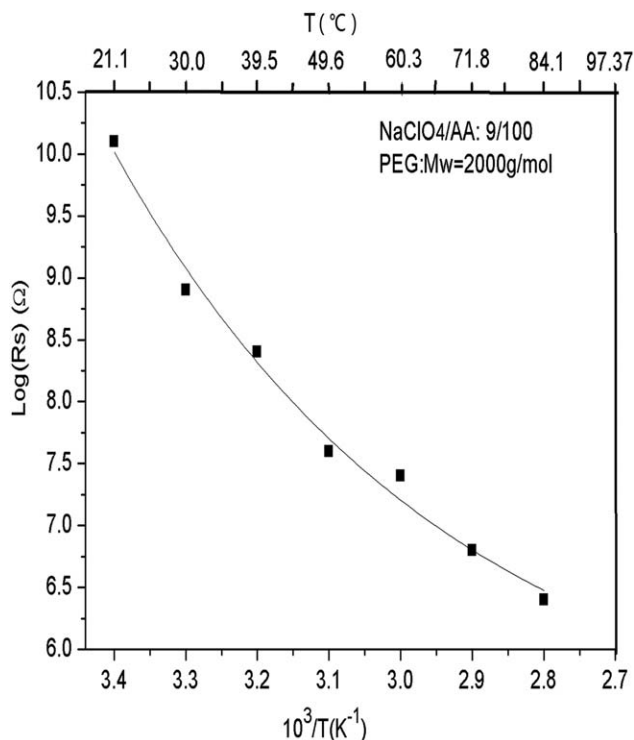


Figure 3. Surface resistivity of APU with different temperature.

between the ether oxygen groups and sodium cations. Meanwhile, increasing temperature enhance the mobility of molecular chains, which is also favorable to ion migration. The dependence of the surface resistivity of the APU on RH at 30°C is displayed in Figure 4. It is clearly illustrated that the surface resistivity of the sample slightly increases with reducing RH, and it only changes within one order of magnitude on

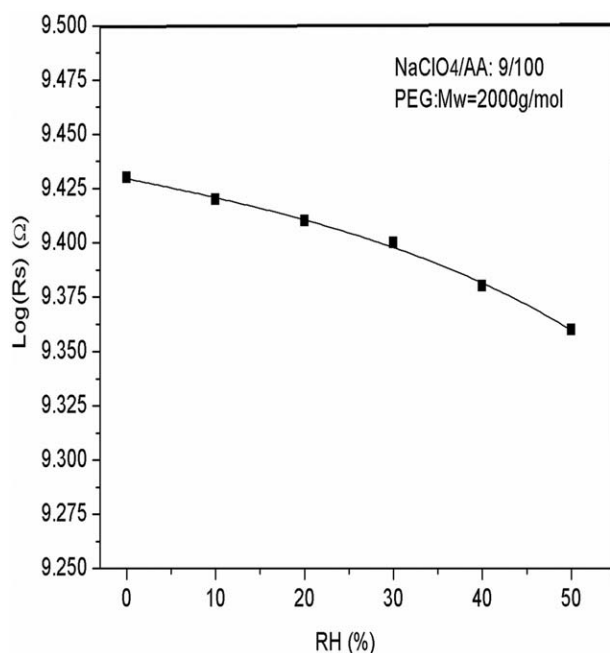


Figure 4. Surface resistivity of APU with different relative humidity (RH).

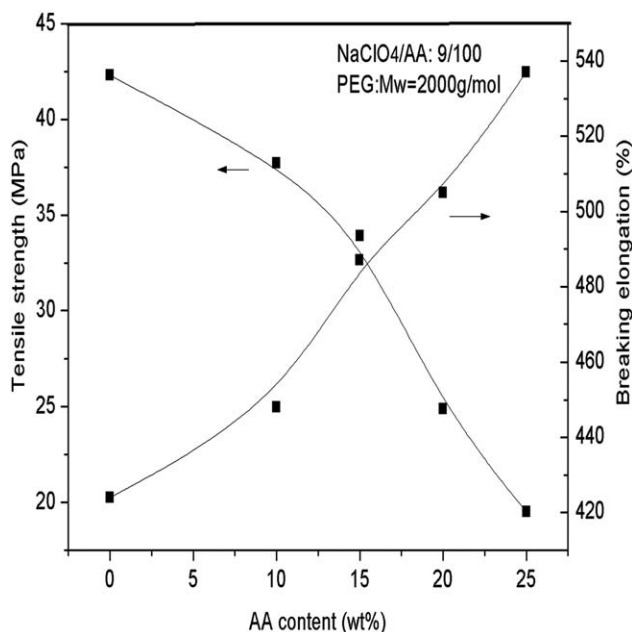


Figure 5. Effect of AA content on the mechanical properties of the APU.

conditions that RH decreases from 50% to 10%, indicating the non-RH-sensitive capacity of the APU. Traditional antistatic agents are apt to migrate to the polymeric surface after processing and could form a conductive water film through the absorption of water in the air. However, the electrolyte-based PEG developed in this study could form conductive networks of tunnels both in polymer matrix and on the surface of the APU. The electrical charges both on the polymeric surface and in the bulk of the matrix are able to leak through the conductive networks or tunnels formed by the PEG-based electrolyte in the APU matrix, in which the alkali salt cations could easily migrate. Therefore, despite the water molecules on the surface of the composites reduced with decreasing RH, the coordination effects between the ether oxygen groups of PEG and Na^+ cations are sufficient to compensate for the loss of the surface water molecules to maintain the APU with a relatively high ion conductivity, even at low RH. Because the surface resistivity of anti-

static materials should be below grade $10^{10} \Omega$,⁴ the APU is still satisfied with antistatic material requirements even under a lower humidity atmosphere.

Mechanical Properties

The mechanical properties are tested in ambient environment, which is designed to find out the effect of AA content on the tensile strength and breaking elongation of APU. As is shown in Figure 5, the tensile strength of APU steeply decreases from around 42.3 to 19.5 MPa while the AA content increases from 0 to 25 wt %, whereas the elongation at break increases from about 424% to 537% with AA contents ranging from 0 to 25 wt %. As it is demonstrated, the introduction of AA reduces the ultimate tensile strength. Compared with polyester glycol (PEL), the cohesion interaction between AA and polymeric matrix is descending. Besides, the introduction of AA reduces the interchain interaction of polymer matrix and lessens the content of hard segments, which adversely affect formation of hydrogen bonds.

Thermogravimetric Results

The effects of PEG and salts on the thermal stability of polymer matrix are shown in Figure 6. As shown in Figure 6(a–c), the introduction of PEG or salts does not bring about considerable change in the initial decomposition temperature of polymer matrix. Different from Figure 6(a), the curves of Figure 6(b) and (c) appear a new decomposition temperature around 370°C caused by degradation of PEG. Moreover, the initial and maximum decomposition temperature of the curve in Figure 6(b) is higher than that of Figure 6(c), implying that the sodium salts are facilitate to the degradation of the polymer matrix. These results can attribute to the reinforcement of ether–urethane interactions with Na^+ ion, leading to more phase mixing of the hard and soft segments, which reduces the number of $-\text{NH}$ groups H-bonded to the carbonyl oxygen in hard area and the cohesion of the APU system. Further, there is no obvious mass loss around 250°C and a few differences to the initial degradation temperature of these curves, exhibiting similar thermal behaviors, indicating that the introduction of PEG or salts has not an apparent effect on the thermal stability of the polymer matrix.

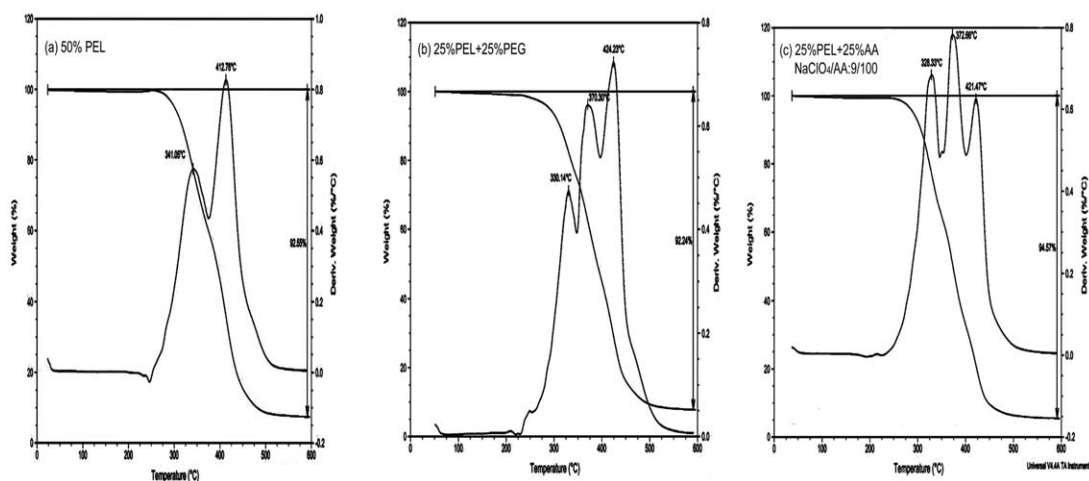


Figure 6. The effect of PEG and salts on thermal stability of polymer matrix.

CONCLUSION

In this study, the APU was successfully prepared by *in situ* polymerization. Temperature had an appreciable effect on the surface resistivity of the APU, which decreases with an increase in temperature. The surface resistivity of the APU gradually reduced with the NaClO₄ content, and declined with increasing the M_w 's of PEG. Though the mechanical properties and thermostability of the APU decreased a little due to the introduction of AA, they could still fulfilled the requirement of processability and application. The surface resistivity of the APU containing 25 wt % AA can be significantly reduced to 10^{9.15} Ω, attaining a practically available antistatic property. Moreover, the study regarding the dependence of the surface resistivity of the APU on the RH showed that the polymers were non-sensitive to the RH.

REFERENCES

1. Jeong, E. H.; Yang, J.; Youk, J. H. *Mater. Lett.* **2007**, 3991.
2. Lee, K. *Macromol. Res.* **2005**, 13, 441.
3. Zhou, X. D.; Liu, P. S. *J. Appl. Polym. Sci.* **2003**, 90, 3617.
4. Grob, M. C.; Minder, E. *Plast. Addit. Comp.* **1999**, 1, 20.
5. Min, C. Y.; Shen, X. Q.; Shi, Z.; Chen, L.; Xu, Z. W. *Polym. Plast. Technol. Eng.* **2010**, 49, 1172.
6. Li, F.; Qi, L.; Yang, J. *J. Appl. Polym. Sci.* **2000**, 75, 68.
7. Chen, G. H.; Wu, C. L.; Weng, W. G.; Wu, D. J.; Yan, W. L. *Polymer* **2003**, 44, 1781.
8. Novak, I.; Krupa, I.; Janigova, I. *Carbon* **2005**, 43, 841.
9. Novak, I.; Krupa, I.; Chodak, I. *Synt. Metals.* **2004**, 144, 13.
10. Yoo, H. J.; Kim, H. H.; Cho, J. W.; Kim, Y. H. *Surf. Interface Anal.* **2012**, 44, 405.
11. Kwon, J. Y.; Koo, Y. S.; Kim, H. D. *J. Appl. Polym. Sci.* **2004**, 93, 700.
12. Yanilmaz, M.; Kalaoglu, F.; Karakas, H.; Sarac, A. S. *J. Appl. Polym. Sci.* **2012**, 125, 4100.
13. Monte, S. J. *Polym. Polym. Compos.* **2002**, 10, 1.
14. Wright, P. V. *Br. Polym. J.* **1975**, 7, 319.
15. Ratner, M. A.; Shriver, D. F. *Chem. Rev.* **1988**, 88, 109.
16. Murate, K. *Electrochim. Acta* **1995**, 40, 2177.
17. MacGlashan, G. S.; Andreev, Y. G.; Bruce, P. G. *Nature* **1999**, 29, 792.
18. Choi, B. K.; Kim, Y. W.; Shin, H. K. *Electrochim. Acta* **2000**, 45, 1371.
19. Saibaba, G.; Srikanth, D.; Reddy, A. R. *Bull. Mater. Sci.* **2004**, 27, 51.
20. Wang, S. W.; Liu, W. J.; Colby, R. H. *Chem. Mater.* **2011**, 23, 1862.
21. Wang, J. L.; Yang, W. Q.; Lei, J. X. *Polym. Eng. Sci.* **2009**, 50, 57.
22. Wang, J. L.; Yang, W. Q.; Lei, J. X. *J. Electrostat.* **2008**, 66, 627.
23. Yang, W. Q.; Wang, J. L.; Lei, J. X. *Polym. Eng. Sci.* **2010**, 50, 739.
24. Wang, J. L.; Yang, W. Q.; Tong, P. C.; Lei, J. X. *J. Appl. Polym. Sci.* **2010**, 115, 1886.
25. Che, R. S.; Yang, W. Q.; Wang, J. L.; Lei, J. X. *J. Appl. Polym. Sci.* **2010**, 116, 1718.
26. Barbosa, P. C.; Rodrigues, L. C.; Silva, M. M.; Smith, M. J.; Parola, A. J.; Pina, F. *Electrochim. Acta* **2010**, 55, 1495.
27. Rajendran, S.; Prabhu, M. R.; Rani, M. U. *J. Appl. Polym. Sci.* **2008**, 110, 2802.
28. Itoh, T.; Horii, S.; Uno, T.; Kubo, M.; Yamamoto, O. *Electrochim. Acta* **2004**, 50, 271.